ISSN 1063-7842, Technical Physics, 2020, Vol. 65, No. 9, pp. 1475–1483. © Pleiades Publishing, Ltd., 2020.
Russian Text © The Author(s), 2020, published in Zhurnal Tekhnicheskoi Fiziki, 2020, Vol. 90, No. 9, pp. 1537–1545.

BIOPOLYMERS DYNAMICS

The Effect of the Concentration of Non-ionic Surfactant Amphiphilic Molecules on the Structure and Gelation in Aqueous Dispersions

S. A. Alekseeva[a,*], I. V. Baranets[a], V. N. Beresnev[a†], T. A. Nadervel[a], A. D. Kryuchkov[a], and T. E. Sukhanova[a]

[a] *S.V. Lebedev Institute of Synthetic Rubber, St. Petersburg, 198035 Russia*

**e-mail: s.alekseeva@fgupniisk.ru*

Received January 9, 2020; revised January 9, 2020; accepted February 17, 2020

Abstract—The structure and morphology of aqueous dispersions, the gelation, and the intermolecular interactions of water molecules with a Synthanol ALM-10 non-ionic low-molecular surfactant have been investigated using viscosimetry, thermogravimetric analysis, IR spectroscopy, and phase-contrast and polarization optical microscopy in the entire range of concentrations (from 0 to 100 wt %). The polymorphism and polydispersity of Synthanol ALM-10 micelles have been detected. We have determined the gelation mechanism in aqueous dispersions containing from 40 to 70 wt % of amphiphilic molecules. It is found that an increase in the concentration in Synthanol ALM-10 dispersions is accompanied, first, with the formation of inverse micelles of the surfactant, followed by sequential alteration of lyotropic mesophases with the hexagonal symmetry and new forms of bound water associated with the formation of clathrate hydrates. The viscosity of the system increases significantly in this case. At high concentrations of Synthanol ALM-10 (exceeding 70 wt %), inverse micelles are mainly observed.

DOI: 10.1134/S1063784220090029

INTRODUCTION

The unique properties of water, which is an important component of biological media that is essential for any living form, have been investigated in a large number of publications of famous scientists (Röntgen [1], Frank and Evans [2], Samoilov [3], Bernal and Fowler [4], Malenkov [5, 24], Pople [6], Pauling [7, 11, 18], Frank and Wen [8], Nemethy and Scheraga [9, 10], Eugene and Stanley [12, 20], Naberukhin [13, 19], Poole et al. [14], Jao et al., [15], Urquidi et al. [16], Tsai and Jordan [17], Zenin [21], Galamba [22], Sarkisov [23], Solovei and Lobyshev [25], and Sidorenko et al. [26]). Nevertheless, the general theory of water structure has not yet been developed.

Analysis of the behavior of water molecules interacting with products of various chemical origins, including surface-active substances (surfactants, SAS), remains a topical problem [27–39]. Surfactants are widely used in paper industry, textile and food industries, in oil extracting and metal processing, in industrial washing and cleaning of solid surfaces, in manufacturing of domestic detergents and hygiene products (soaps, shampoos, creams, and toothpastes), and in pharmacology and medicine (e.g., in manufacturing of soft drugs and hydrogel bandage for healing wounds and burns). In addition, surfactants are indispensable in various chemical processes as a medium for separating substances in chromatography [33–35], as emulsifiers for emulsion polymerization of rubbers [36–38], and in obtaining bitumen emulsions for asphalt coatings of roads and for roof coating [39].

Among commercial surfactants, Synthanols (oxyethylated alcohols) are mixtures of polyethylene glycol esters differing in the numbers of oxyethylene groups and in the size of a hydrophobic radical. The structural theory explains the solubility of polyethylene glycols (PEGs) in water by the closeness of the length of the O–O bonds in the hexagonal structure of ice (0.274 nm) and in PEG (0.276 nm), which makes it possible to replace water molecules by oxygen atoms of PEG molecules.

This study is aimed at analysis of self-organization process of SAS amphiphilic molecules and water molecules depending on the SAS concentration in aqueous dispersions, as well as the structure and morphology of gels being formed.

1. EXPERIMENTAL

The objects of investigation were aqueous dispersions of Synthanol ALM-10 non-ionic low molecular surfactant in a wide range of concentrations (from 3

† Deceased.

Table 1. Phase-transition temperatures of the SAS/water system obtained by the TGA method

SAS/water ratio, wt %	Decomposition steps, °C	Final decomposition temperature, °C	Phase-transition temperatures °C
0/100	90	98	84–90
10/90	93–118	391	81–359
20/80	87–160–377	411	83–88–388
30/70	93–103–155–384	425	80–101–106–400
40/60	85–156–252	429	83–403
50/50	94–168–408	433	81–108–401–408
60/40	80–96–172	424	85–111–387–403
70/30	95–109–122–169–249	441	72–114–127–249–405
80/20	78–164	436	59–407
90/10	195	431	48–124–408
100/0	197	440	407

to 95 wt %) with a step of 3–5 wt %, which were obtained at room temperature. Prior to mixing, the SAS paste was heated in a water bath at +70°C for 15 min for eliminating the previous history of the sample (crystallization during storage). The initial material (Synthanol ALM-10) consists of amphiphilic molecules of oxyethylated alcohol $C_nH_{(2n+1)}O(C_2H_4O)_m$, where n = 10–13 is the carbon chain length and m = 10 is the degree of ethoxylation. The molecular mass is 362.54 g/mol. The storage time for distilled water prior to the preparation of dispersions did not exceed three days.

The structural–morphological experiments with SAS aqueous dispersions were performed using the methods of phase-contrast and polarization microscopies in an analytical complex including a Leica DM-2500 optical research microscope, a Leica DFC-420 digital color camera, and the Leica Application Suite specialized computer station and software. Thin layers of water dispersions ("live drops") between the cover and object glasses were analyzed "in transmission" in the wavelength range from 200 to 1200 nm, including near ultraviolet, visible light, and infrared radiation. The main results of investigations were obtained in the form of microphotographs.

The phase-transition temperatures for aqueous dispersions with different concentrations were determined using thermogravimetric analysis (TGA) on a STA 6000 device (Perkin Elmer). The samples were heated in the temperature interval from 20 to 500°C at a rate of 10°C/min with continuous fixation of the sample mass loss to within $\pm 10^{-4}$ mg and variation of the heat flux [mW] and the mass loss rate [mg/min] depending on temperature. The results of investigation are given in Table 1.

The variation of the dynamic viscosity of aqueous dispersions for each SAS/water ratio was investigated at a temperature of +25 ± 0.03°C in the shear rate range from 1.5 to 125 s^{-1} on a Discovery Hybrid Rheometer-1 (TA Instruments, United States). The values of viscosity of aqueous dispersions under a shear rate of 34.36 s^{-1} were used for plotting the dependence of the dispersion viscosity on the SAS content. This parameter was chosen because the viscosity of water obtained in these conditions corresponds to tabulated values.

The IR spectra were obtained using a Spectrum 100 infrared Fourier spectrometer (Perkin Elmer, United States) equipped with an attachment of frustrated total internal reflection (FTIR) with a diamond crystal. The scanning range was from 650 to 4000 cm^{-1} with a resolution of 4 cm^{-1}.

2. RESULTS AND DISCUSSION

The structural–morphological investigations of Synthanol ALM-10 in the initial state of the material revealed the presence of spherical diffusive associates formed as a result of merging of direct and inverse micelles consisting of SAS amphiphilic molecules (Fig. 1a) with diameters varying from 0.3 to 1.3 μm. Chain structures of optically dense spherical associates can also be clearly seen on microphotographs (see Fig. 1a).

The hydrophilic part of the Synthanol ALM-10 molecule containing oxygen atoms exhibits a higher optical density as compared to the hydrophobic "tail" containing carbon links [40]. In direct SAS micelles, the hydrophilic parts of molecules (with oxygen atoms) are located at the periphery of micelles; for this reason, direct micelles have a higher optical activity (appear as dark regions on the microphotographs) than "inverse" micelles (light circular formations), in which hydrophobic fragments of molecules are located at the periphery.

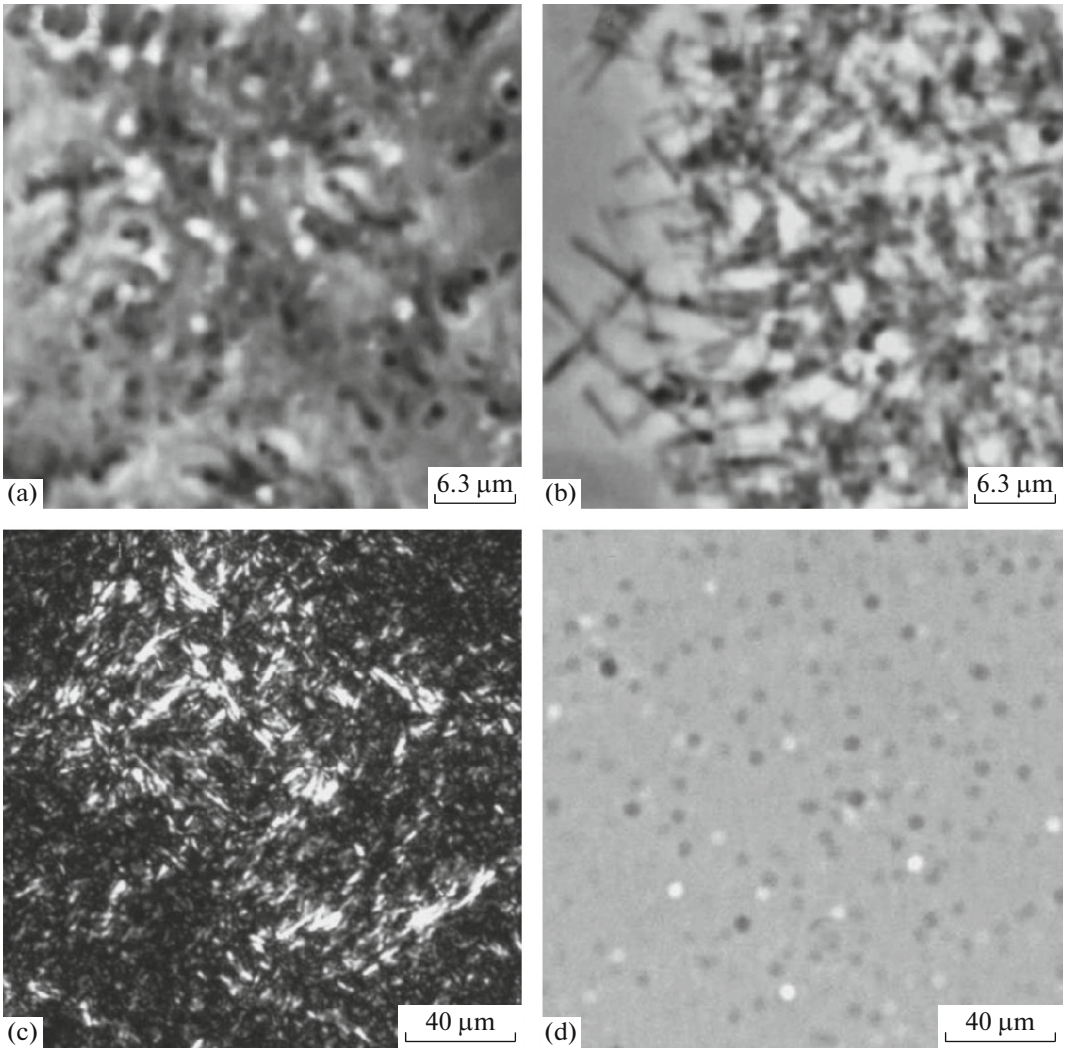

Fig. 1. (a, b, c) Microphotographs of initial Synthanol ALM-10 in the viscous-flow state and (d) of aqueous dispersion containing 90 wt % SAS obtained in (a, b, d) phase contrast and (c) crossed nicols regimes.

In Synthanol ALM-10 samples, cylindrical micelles with quite coarse rod-like particles of diameter from 0.4 to 0.9 μm and with a length from 1.8 to 13.5 μm are formed with time because of intermicellar interactions (Fig. 1b). After prolonged storage (for more than three months at room temperature), analysis in "crossed nicols" revealed the characteristic birefringence indicating the formation of a long-range order in packing of Synthanol ALM-10 molecules both in spherical and cylindrical supermolecular formations (Fig. 1c). Spherical associates consisting of direct and inverse micelles with an average size of 4.5 μm were detected in the aqueous dispersion containing 90 wt % SAS (Fig. 1d).

For low SAS contents (up to 6 wt %), only individual micelles exist in the aqueous solution, while supermolecular structures with a size exceeding 100 nm are absent. For an SAS content exceeding 6 wt % (the critical micelle-formation concentration (CMC) for Synthanol ALM-10), diffuse spherical associates of direct micelles appear in the solution. For an SAS content of 10 wt %, their diameter varies from 200 to 800 nm (Fig. 2a).

For a SAS content of 20 wt %, a skeleton of cyclic structures (Fig. 2) resembling a microtrabecular structure of a living cell is formed [41]. The diameter of supermolecular formations varies from 0.8 to 2.9 μm.

For an SAS content of 25 wt %, the formation of a filamentary network with a "pearl necklace" morphology was detected [42]; it consists of spherical particles with an average diameter of 6.1 μm (Fig. 2c). This effect can be due to enhanced structuring of water in the nearest surrounding of SAS macromolecules. For a Synthanol ALM-10 concentration of 30 wt %, the mutual ordering of molecules in aqueous dispersion is enhanced, and supermolecular formations resembling dendrites appear (Fig. 2d).

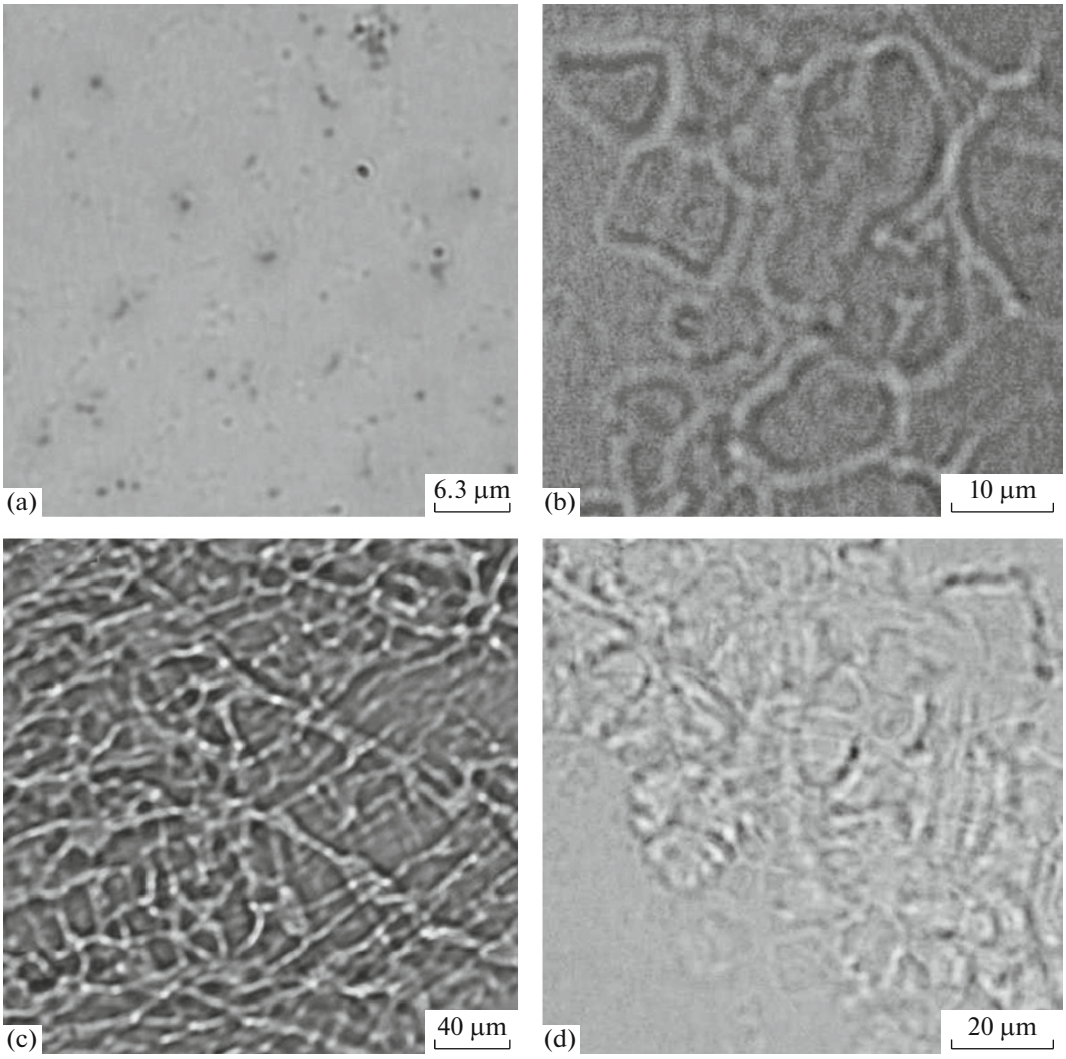

Fig. 2. Microphotographs of aqueous dispersions with Synthanol ALM-10 concentrations of (a) 10, (b) 20, (c) 25, and (d) 30 wt % obtained in a phase contrast regime.

However, analysis of these compositions in the "crossed nicols" regime did not reveal birefringence. In analysis of aqueous dispersions in the crossed nicols regime, supermolecular structure exhibiting birefringence are present in samples with concentrations from 35 to 70 wt % (Figs. 3, 4). For a Synthanol ALM-10 concentration of 35 wt %, clusters of cylindrical direct and inverse micelles are formed in aqueous dispersions (Figs. 3a, 3b). The sizes of birefringence zones in this compound vary from 6.4 to 51.3 μm that alternate with amorphous regions and do not form a single frame.

Upon a further increase in the SAS content to 45 wt %, a fan-shaped texture is formed in the liquid phase (Fig. 3c). Simultaneously, a gel is intensely formed. The gel is characterized by the so-called "broken fan-shaped texture" (Fig. 3d) with a hexagonal supermolecular organization of the mesophase [43].

In a Synthanol ALM-10 concentration range of 50–70 wt %, the fan-shaped texture is perfected (the sizes of mesomorphic domains with identically oriented macromolecular formations increase; Figs. 4a–4c).

For a SAS content of 75 wt %, microphotographs clearly illustrate a layered lamellar morphology of the sample (Fig. 4d). It should be noted that the structure of lamellas varies in the birefringence intensity of the ends and surfaces: we can see some lamellas in which birefringence (and, hence, crystallographic order) is stronger on the lamella surface, while the lamella end does not exhibit birefringence. On the other hand, the ends of other lamellas demonstrate strong birefringence. We probably observe lamella clusters of direct and inverse micelles in the aqueous frame. Therefore, fan-shaped liquid-crystal textures are formed in aqueous dispersions with a SAS content from 35 to 70 wt %.

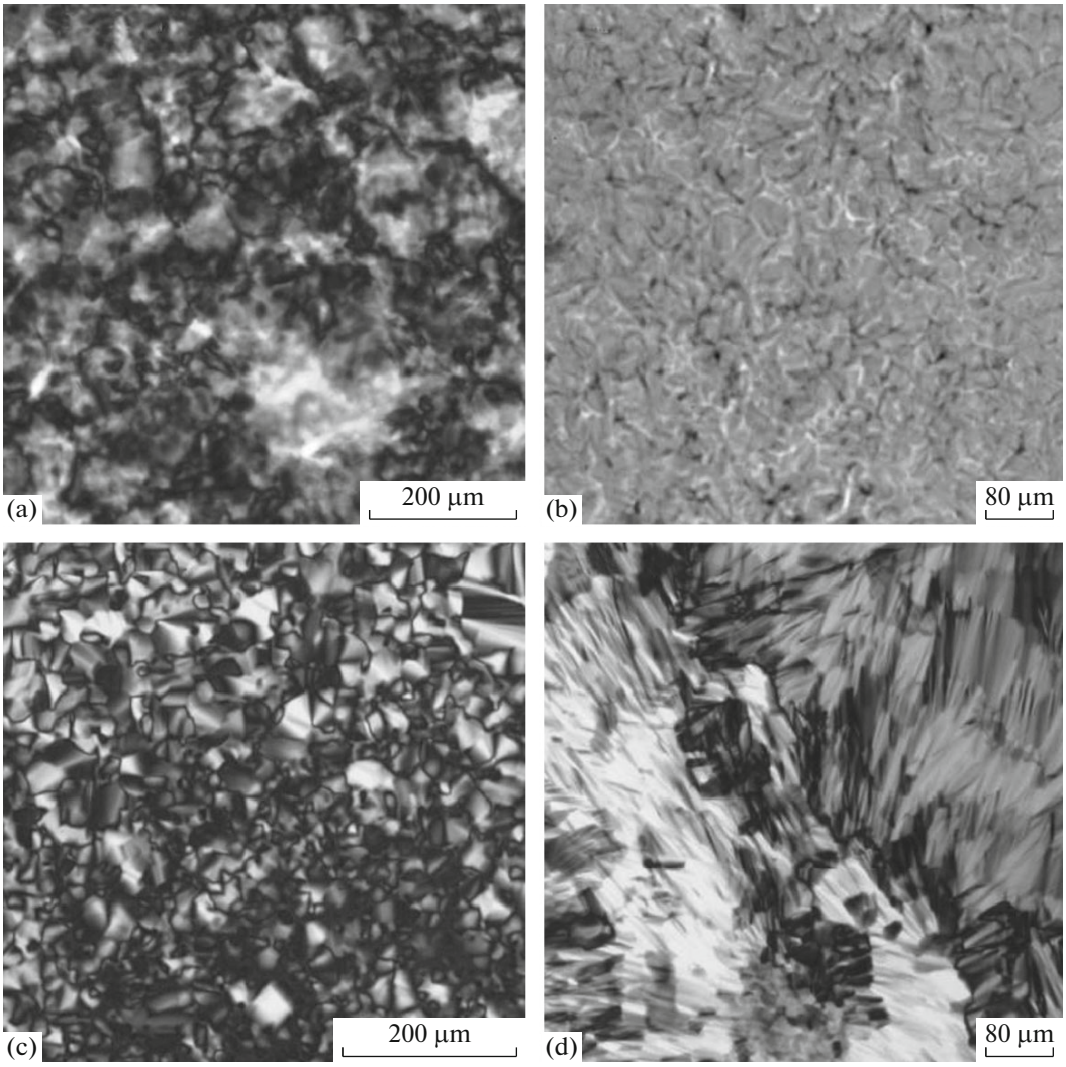

Fig. 3. Microphotographs of aqueous dispersions with Synthanol ALM-10 concentrations of (a, b) 35 and ((c) liquid phase, and (d) gel) 45 wt % obtained in (a, c, d) crossed nicols and (b) phase contrast regimes.

For a Synthanol ALM-10 concentration of 80–90 wt %, no liquid-crystal phase was detected in solutions and gelation did not occur. It can be seen on the microphotograph that such samples contain diffuse spherical clusters consisting predominantly of inverse micelles of diameter from 2.8 to 7.3 μm (see Fig. 1d).

For determining the phase-transition temperatures in Synthanol ALM-10 solutions upon a change in the concentration, aqueous dispersions and initial substances (distilled water and Synthanol ALM-10) were investigated by the TGA method. The main results are compiled in Table 1.

It can be seen from the table that initial distilled water experiences two phase transition, which confirms the hypothesis of a two-structure model of water [1, 2, 4, 5, 15, 24], and Synthanol ALM-10 experiences one phase transition at 407°C. Two phase transitions are observed in aqueous dispersions for an SAS content up to 10 wt %. In this case, the final decomposition temperature and the phase-transition temperature decrease significantly as compared to these characteristics for Synthanol ALM-10 (by 49 and 48°C, respectively), indicating the intermolecular interaction between the SAS and water molecules.

A further increase in the concentration of SAS aqueous dispersions is accompanied with a shift of the low-temperature phase transition from 84°C (for water) to 48°C (in the dispersion with 90 wt % SAS), as well as the high-temperature phase transition of water toward positive temperatures (from +90 to +114°C for a SAS content of 70 wt %). Such a behavior of solutions indicates the reorganization of two types of the supermolecular structure of water molecules interacting with the surfactant.

It is interesting that, upon an increase in the SAS content from 20 to 70 wt %, the number of phase tran-

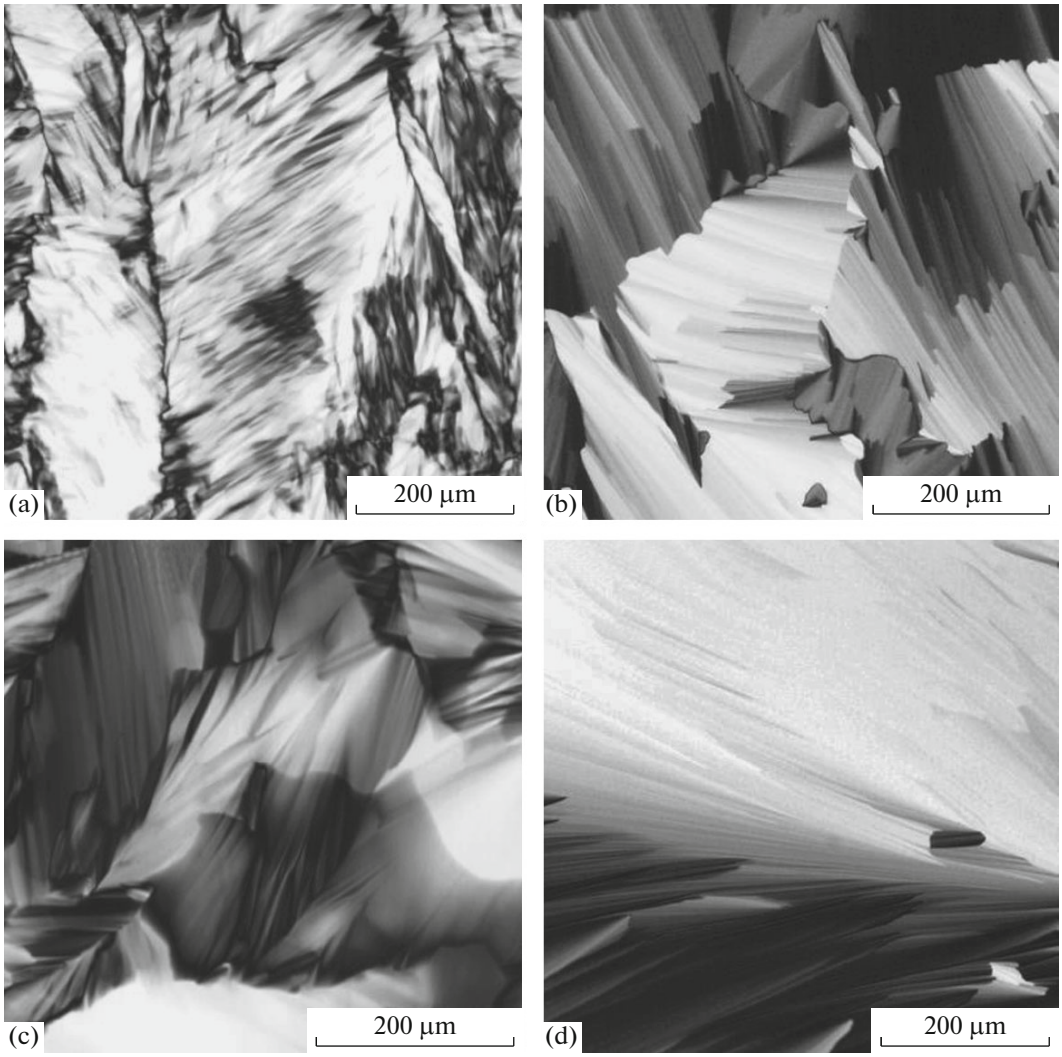

Fig. 4. Microphotographs of aqueous dispersions with Synthanol ALM-10 concentrations of (a) 50, (b) 55, (c) 60, and (d) 70 wt % obtained in a crossed nicols regime.

sitions in aqueous dispersions increases. For an SAS content of 70 wt %, five types of mesomorphic structures are formed sequentially with different degrees of ordering because of the interaction of molecules of water and Synthanol ALM-10, which is in good agreement with the results of morphological analysis of these systems (see Figs. 2–4). For Synthanol ALM-10 concentrations of 80 and 90 wt % in aqueous dispersions, the position of phase transitions on the temperature scale remains almost unchanged.

The variation of segmental interactions in Synthanol ALM-10 aqueous dispersions was estimated using infrared spectroscopy. The distilled water spectrum (Fig. 5a) has two peaks at frequencies of 1638 and 3500 cm^{-1}, which is in conformity with the results of thermogravimetric analysis. The broad bell-shaped peak lying at a frequency of 3500 cm^{-1} contains stable spectral components corresponding to hexagonal ice (3200 cm^{-1}), small-size complexes (3450 cm^{-1}), and (to a lesser extent) monomers (3650 cm^{-1}).

In the spectrum of initial Synthanol ALM-10 (Fig. 5b), the main peak lies near 1100 cm^{-1}. The positions on the frequency scale and the shape of extrema of the IR-spectra of the initial components and aqueous dispersion for an SAS content of 6 wt %, which corresponds to the critical concentration of micelle formation, coincide (Figs. 5a, 5b, 5d). Therefore, no intermolecular interaction between Synthanol ALM-10 and water were detected at this concentration of aqueous dispersions.

Figure 5c shows the IR-spectrum of aqueous dispersion containing 60 wt % SAS and having a gel-like consistence. For this system, additional intermolecular interaction bands near 2900–3000 and 1200–1500 cm^{-1} and a sharp increase in the absorption peak height near 1100 cm^{-1} were observed. The bell-shaped

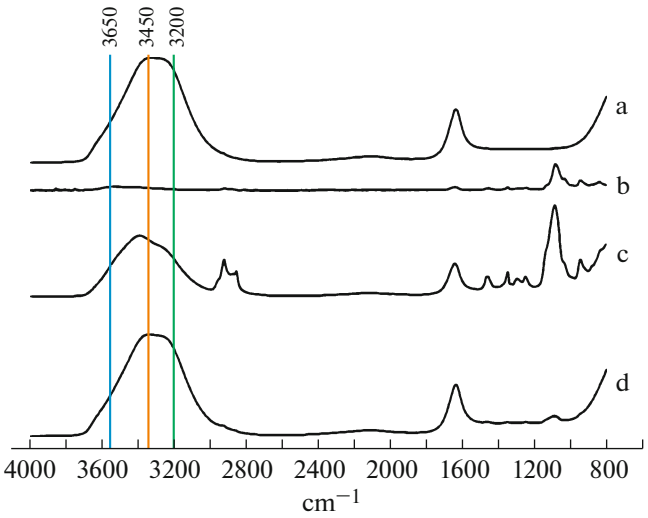

Fig. 5. IR spectra of (a) distilled water, (b) initial Synthanol ALM-10, (c) aqueous dispersion containing 60 wt % of Synthanol ALM-10, and (d) aqueous dispersion containing 6 wt % of Synthanol ALM-10.

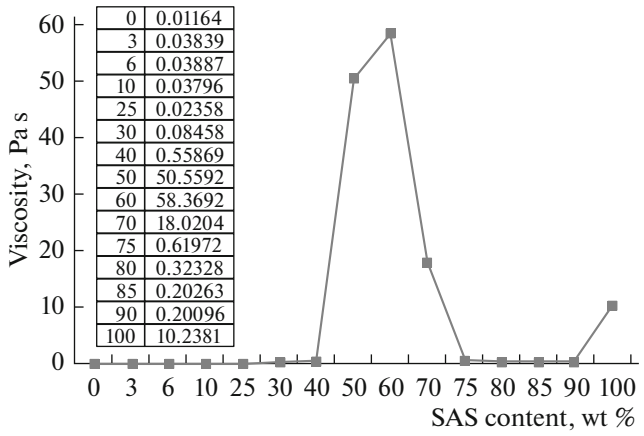

0	0.01164
3	0.03839
6	0.03887
10	0.03796
25	0.02358
30	0.08458
40	0.55869
50	50.5592
60	58.3692
70	18.0204
75	0.61972
80	0.32328
85	0.20263
90	0.20096
100	10.2381

Fig. 6. Dependence of the dynamic viscosity of aqueous dispersion of Synthanol ALM-10 on SAS content at a shear rate of 34.36 s^{-1}.

peak also changed simultaneously (the intensity of absorption at 3200 cm^{-1} typical of hexagonal ice decreases). These results indicate an active intermolecular interaction of water and Synthanol ALM-10 molecules.

For each SAS/water ratio, we measured the dynamic viscosity and plotted the corresponding dependences. For each sample, we chose the values of the solution viscosity for a shear rate of 34.36 s^{-1}. From the chosen values, we plotted the graph describing the dependence of viscosity on the SAS content (Fig. 6). The numerical values of viscosity for a chosen shear rate are given in the table in the right part of the figure.

It was found that the viscosity of the samples demonstrated the maximal increase in the range from 40 to 70 wt % SAS. Aqueous dispersions had a gel-like consistence for Synthanol ALM-10 concentrations from 45 to 70 wt %, while the fan-shaped mesomorphic texture with different degrees of ordering was detected in the concentration interval from 35 to 70 wt % SAS.

In our opinion, the reason for gelation of SAS aqueous dispersions is the formation of clathrate hydrates [44] consisting of a frame formed by water molecules fixed by hydrogen bonds around Synthanol ALM-10 macromolecules.

Analysis of the available models of the interaction between water and amphiphilic SAS molecules reveals that the model proposed by Galamba [22] in 2013 (Fig. 7), in which the scheme of intermolecular interactions in the vicinity of hydrophobic substances has been considered using molecular-dynamic simulation, is the closest to the processes discovered in our study. This model is the development of the Iceberg model formulated earlier by Frank and Evans [2].

Thus, we discovered the effect on each other of water and an SAS molecule on the morphology and the degree of ordering of supermolecular formations. The parameter determining the formation of direct or inverse spherical or cylindrical micelles (cyclic structures or mesomorphic textures) is the SAS/water ratio. This circumstance must be taken into account because local changes in the SAS content in aqueous dispersions are possible (e.g., in the absorption layer of polymer–monomer particles during emulsion polymerization [37, 38] or on the surface of impurities in multicomponent systems for other applications).

CONCLUSIONS

1. We have investigated self-organization of aqueous dispersions of non-ionic amphiphilic surfactant Synthanol ALM-10 upon a change in its concentration in a wide range.

2. Using dynamic viscosimetry, we detected extremal increase in the viscosity of aqueous dispersions of Synthanol ALM-10 in the concentration range from 40 to 70 wt %.

3. Gelation (i.e., the formation of a spatial ensemble of mutually ordered molecules) was detected in a concentration range of 45–70 wt %, while the formation of mesomorphic structure (fan-shaped texture with different degrees of ordering) was observed in SAS aqueous dispersions in the concentration range from 35 to 70 wt %.

4. Morphological investigations also revealed the presence of predominantly direct micelles at low SAS contents (up to 30 wt %). In the concentration interval from 35 to 70 wt %, direct and inverse SAS micelles incorporated in mesomorphic structures are observed,

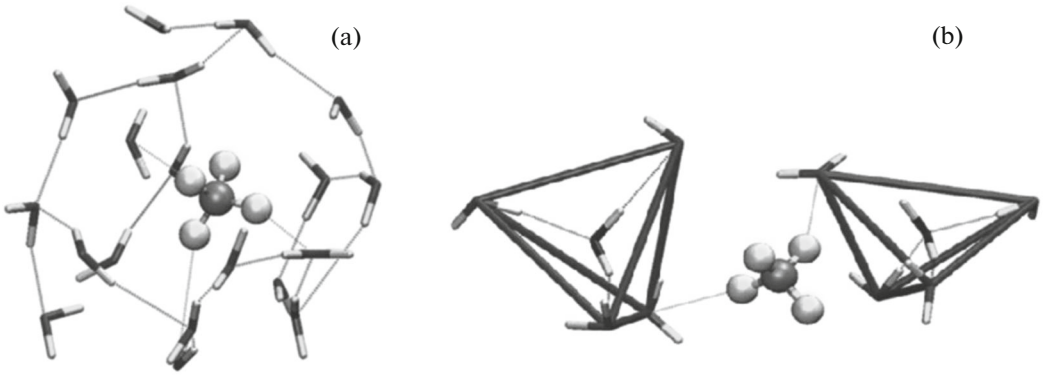

Fig. 7. Snapshots of aqueous CH_4 showing (a) water's "cage" around methane, corresponding to the water molecules in the first hydration shell, and (b) two water pentamers forming nearly perfect regular tetrahedra, with the central water molecule and water molecules at the four vertices [22].

while predominantly inverse micelles are present for higher SAS contents (exceeding 70 wt %).

5. TGA and IR studies of aqueous dispersions of Synthanol ALM-10 revealed that an increase in the SAS content is accompanied with the emergence of new forms of bound water and the formation of clathrate hydrates.

ACKNOWLEDGMENTS

The authors are grateful to I.V. Kokotin (Federal State Unitary Enterprise S.V. Lebedev Institute of Synthetic Rubber) for his help in recording IR spectra.

CONFLICT OF INTERESTS

The authors declare that they have no conflicts of interest.

REFERENCES

1. W. C. Röntgen, Ann. Phys. Chem. N.F. **45**, 91 (1891).
2. H. S. Frank and M. W. Evans, J. Chem. Phys. **13**, 507 (1945).
3. O. Ya. Samoilov, *Structure of Aqueous Electrolytes and Hydration of Ions* (Akad. Nauk SSSR, Moscow, 1957), pp. 173–180 [in Russian].
4. J. D. Bernal and R. H. Fowler, J. Chem. Phys. **1**, 515 (1933).
5. G. G. Malenkov, J. Phys.: Condens. Matter **21**, 6 (2009).
6. J. A. Pople, Proc. R. Soc. London, Ser. A **205**, 163 (1951).
7. L. Pauling, *The Hydrogen Bonding*, Ed. by D. Hadji (Pergamon, Oxford, 1959).
8. H. S. Frank and W. Y. Wen, Discuss. Faraday Soc. **24**, 133 (1957).
9. G. Nemethy and H. A. Scheraga, J. Chem. Phys. **36**, 3382 (1962).
10. G. Nemethy and H. A. Scheraga, J. Chem. Phys. **36**, 3401 (1962).
11. L. Pauling, *The Nature of the Chemical Bond* (Cornwall Univ. Press, New York, 1939).
12. H. E. Stanley and J. Teixeira, J. Chem. Phys. **73**, 3404 (1980).
13. Yu. I. Naberukhin, J. Struct. Chem. **33** (6), 772 (1993).
14. P. H. Poole, F. Sciortino, U. Essmann, and H. E. Stanley, Nature **360**, 324 (1992).
15. H. Jao, J. Lee, and G. W. Robinson, J. Am. Chem. Soc. **112**, 5698 (1990).
16. J. Urquidi, S. Singh, C. H. Cho, and G. W. Robinson, Phys. Rev. Lett. **83**, 2348 (1999).
17. C. J. Tsai and K. D. Jordan, J. Phys. Chem. **97**, 5208 (1993).
18. L. Pauling, J. Am. Chem. Soc. **57**, 2680 (1935).
19. Yu. I. Naberukhin, Soros. Obraz. Zh., No. 5, 41 (1996).
20. H. E. Stanley, MRS Bull. **24** (5), 22 (1999).
21. S. V. Zenin, Doctoral Dissertation in Biology (Inst. Med. Biol. Problems, Moscow, 1999).
22. N. Galamba, J. Chem. Phys. B **117** (7), 2153 (2013).
23. G. N. Sarkisov, Phys.-Usp. **49** (8), 809 (2006).
24. G. Malenkov, J. Phys.: Condens. Matter **21** (28), 283101 (2009).
25. A. B. Solovei and V. I. Lobyshev, Russ. J. Phys. Chem. A **80** (10), 1578 (2006).
26. O. E. Sidorenko, E. K. Ivanova, B. L. Oksengendler, and N. N. Turaeva, Kondens. Sredy Mezhfaz. Granitsy **13** (3), 341 (2011).
27. A. V. Karyakin and G. A. Kriventsova, *State of Water in Organic and Inorganic Compounds* (Nauka, Moscow, 1972) [in Russian].
28. *Water in Polymers*, Ed. by S. P. Rowland (Am. Chem. Soc., Washington, 1980).
29. D. A. Zherebtsov, Vestn. Yuzhno-Ural. Gos. Univ., Ser. Metallurgiya **19** (3), 66 (2019).
30. R. E. Neiman, V. N. Varezhnikov, A. P. Kirdeeva, O. G. Kiseleva, I. N. Lebedeva, and O. A. Lyashenko, *Workshop on Colloidal Chemistry of Latex and Surfactants: Handbook for Universities*, Ed. by R. E. Neiman (Vysshaya Shkola, Moscow, 1972) [in Russian].

31. O. P. Mchedlov-Petrosyan, A. V. Lebed', and V. I. Lebed', *Colloidal Surfactants: A Textbook* (Karazin Kharkov Nats. Univ., Kharkov, 2009) [in Russian].
32. E. E. Bibik, *Colloidal Solutions and Suspensions. Guide to Action: Handbook with CD-ROM* (Professiya, St. Petersburg, 2018) [in Russian].
33. S. N. Shtykov, J. Anal. Chem. **55** (7), 608 (2000).
34. D. W. Armstrong and J. H. Fendler, Biochim. Biophys. Acta **478** (2), 75 (1977).
35. S. E. Porozova, *Surfactants in Sol-Gel Technology: Handbook* (Perm Nat. Res. Polytech. Univ., Perm, 2014) [in Russian]. ISBN 978-5-398-01198-2
36. V. N. Beresnev, Candidate's Dissertation (Lensovet Leningrad Technol. Inst., Leningrad, 1966).
37. V. N. Beresnev, I. I. Kraynik, and I. V. Baranets, *Proc. 7th All-Russ. Kargin Conf. "Polymers-2017", Moscow, Russia, June 13–17, 2017*, p. 135 [in Russian].
38. V. N. Beresnev, I. I. Kraynik, I. V. Baranetc, and L. V. Agibalova, Russ. J. Appl. Chem. **91** (7), 64 (2018).
39. K. R. Lange, *Surfactants: A Practical Handbook* (Hanser, Munich, 1999).
40. E. Pretsch, P. Bühlmann, and C. Affolter, *Structure Determination of Organic Compounds. Tables of Spectral Data* (Springer, Berlin, 2000). https://doi.org/10.1007/978-3-662-04201-4
41. A. A. Vedenov and E. B. Levchenko, Sov. Phys.-Usp. **26** (9), 747 (1983). https://doi.org/10.1070/PU1983v026n09ABEH004490
42. A. V. Ten'kovtsev, T. E. Sukhanova, M. E. Kompan, V. A. Lukoshkin, A. E. Bursian, and M. P. Perminova, Phys. Solid State **51** (3), 620 (2009). https://doi.org/10.1134/S1063783409030305
43. T. E. Sukhanova, A. I. Grigoriev, et al., in *Polyimides and Other High Temperature Polymers*, Ed. by K. L. Mittal (VSP, The Netherlands, 2007), Vol. 4, pp. 47–66.
44. M. Kh. Karapetyants and S. I. Drakin, *The Structure of Matter* (Central Books, London, 1974).

Translated by N. Wadhwa